

The Ionic Expression Gradients affect Paroxysmal Atrial Fibrillation Dynamics: A Simulation Study

Catalina Tobón¹, Karen Cardona², Sandeep V Pandit³, José Jalife³, Omer Berenfeld³, Javier Saiz²

¹GI2B, Instituto Tecnológico Metropolitano, Medellín, Colombia

²I3BH, Universitat Politècnica de València, Valencia, Spain

³Center for Arrhythmia Research, University of Michigan, Ann Arbor, USA

Abstract

Ionic expression gradients could determine the paroxysmal atrial fibrillation (pAF) dynamics. Recently, it has been demonstrated that the acetylcholine (ACh)-activated potassium current ($I_{K_{ACh}}$) and the inward rectifier K^+ current (I_{K1}) densities are ≈ 2 -fold larger in the left atrium (LA) versus right atrium (RA) during pAF, which may result in a greater increase in LA than RA rotor frequency. We investigated how the ionic expression gradients may affect the pAF dynamics. Experimental LA-RA I_{K1} and $I_{K_{ACh}}$ gradients were incorporated in a cellular atrial kinetics to simulate pAF in a 3D model of the human atria. pAF episodes were generated by a burst of 6 ectopic beats. In pAF model (with I_{K1} and $I_{K_{ACh}}$ gradients) action potential duration (APD) gradient was observed. However, without I_{K1} gradient or without $I_{K_{ACh}}$ gradient the APD gradient was decreased. In the pAF model, single rotor and then figure-of-eight reentry sustained in the LA maintained the AF, without reentrant activity in RA. When one of the two ionic expression gradients was not present, the pAF was maintained by multiple reentrant waves that collided and fragmented in the RA. In conclusion, LA-RA gradients in both $I_{K_{ACh}}$ and I_{K1} expression are important in establishing APD and frequency gradients, and LA reentrant activity maintaining pAF.

1. Introduction

Atrial arrhythmias, in particular atrial fibrillation (AF), are the most prevalent cardiac arrhythmia. While not directly lethal, AF provokes disabling symptoms and severe complications such as heart failure and stroke [1]. Paroxysmal atrial fibrillation (pAF) may occur in episodes lasting from minutes to days. If the pAF is not treated it could become permanent. Experimental and clinical evidence suggest that certain cases of AF are maintained by high frequency small reentrant sources (rotors) that result in a hierarchical distribution of

frequencies throughout the atria.

Recently, it has been demonstrated that the acetylcholine (ACh)-activated potassium current ($I_{K_{ACh}}$) and the inward rectifier K^+ current (I_{K1}) densities are ≈ 2 -fold larger in the left atrium (LA) versus right atrium (RA) during pAF [2] which may result in a greater increase in LA than RA rotor frequency [3] and dynamic changes.

In this work, we use computational 3D human atrial models to study how gradients in I_{K1} and $I_{K_{ACh}}$ expression may affect the pAF dynamic.

2. Methods

2.1. Model of human atria

We implemented a three-dimensional model of human atria developed previously [4]. The model including realistic fiber orientation and anisotropy, and comprises the main anatomical structures: left and right atrial chambers (LA and RA), the crista terminalis (CT), pectinate muscles (PM), left and right appendages (LAPG and RAPG), left and right pulmonary veins (LPV and RPV), superior and inferior caval veins (SCV and ICV), the coronary sinus (CS) and atrioventricular rings (AVR). The sinoatrial node (SAN) is situated near the ostium of the SCV. The model includes three different pathways for inter-atrial conduction of electrical propagation: the Bachmann's bundle (BB), limbus of the fossa ovalis (FO) and discrete sites of the CS (Figure 1).

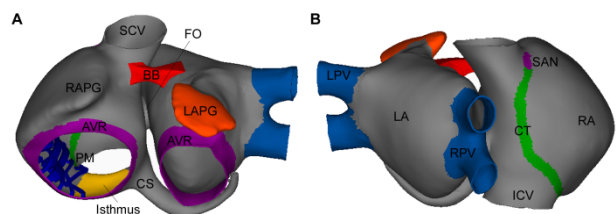


Figure 1. A) Anterior and B) posterior view of the 3D model of human atria.

One of the characteristics of the atrial model is the realistic fiber orientation included based on histological observations [5].

2.2. Model of action potential propagation

The Courtemanche-Kneller atrial kinetics [6,7] was used to reproduce the cellular electrical activity. The electrophysiological heterogeneity reported by Feng et al. [8] was included to reproduce action potentials in different parts of the atria.

The monodomain model of the electrical propagation of AP along the tissue model is described by the following reaction-diffusion equation:

$$\frac{1}{S_v} \nabla \cdot (D \nabla V_m) = C_m \frac{\partial V_m}{\partial t} + I_{ion} - I_{stim} \quad (1)$$

where C_m is the specific membrane capacitance, V_m is the membrane potential, I_{ion} is the total ionic current that crosses the membrane cells, I_{stim} is the stimulus current, D is the conductivity tensor and S_v corresponds to the surface-to-volume ratio. Equations were numerically solved using Finite Element Method.

2.3. Model of pAF

Experimental LA-RA I_{K1} and I_{KACH} gradients [2,3] were incorporated in the CRN-Kneller atrial kinetics to simulate pAF in a 3D model of the human atria under the presence of $0.005 \mu\text{M}$ ACh. I_{KACH} and I_{K1} currents were 2-fold larger in LA than in RA cardiomyocytes. To study how the ionic expression gradients affect the pAF dynamic, we built different pAF models (see Table 1):

1. pAF with LA-RA I_{K1} and I_{KACH} gradients.
2. pAF with LA-RA I_{KACH} gradient, without I_{K1} gradient.
3. pAF with LA-RA I_{K1} gradient, without I_{KACH} gradient.

Table 1. Ionic current changes (in %) in LA and RA to develop the pAF models.

Model	I_{K1}		I_{KACH}	
	LA	RA	LA	RA
pAF	↑100%	-	↑100%	-
pAF without I_{K1} gradient	-	-	↑100%	-
pAF without I_{KACH} gradient	↑100%	-	-	-

“-” means no change.

2.4. Simulation protocol

pAF episodes were generated by S1-S2 protocol as

follows: a train of stimuli with a basic cycle length (BCL) of 500 ms was applied during 5 seconds in the SAN area to simulate the sinus rhythm (S1). After the last beat of the sinus nodal stimulus, a burst of 6 ectopic (S2) to high frequency was delivered into the superior beats in the right superior pulmonary vein. All simulations were completed within 5 seconds.

2.5. Unipolar electrograms

Unipolar electrograms, at 2 mm from the surface, were simulated. The extracellular potential (Φ_e) is given by the following equation:

$$\Phi_e(r) = -\frac{1}{4\pi} \frac{\sigma_i}{\sigma_e} \iiint \nabla V_m(r') \cdot \nabla' \left[\frac{1}{r'-r} \right] dv \quad (2)$$

where ∇V_m is the spatial gradient of transmembrane potential, σ_i is the intracellular conductivity, σ_e is the extracellular conductivity, r is the distance from the source point (x, y, z) to the measuring point (x', y', z') and dv is the differential volume.

Spectral analysis of the signals was performed with a Fast Fourier transform. The dominant frequency (DF) corresponding to the highest peak in the power spectrum was calculated.

3. Results

In the pAF model with I_{K1} and I_{KACH} gradients, the action potential duration (APD) gradient observed between two points at the free LA and RA walls was 53%. However, without I_{K1} gradient the APD gradient was decreased to 39%, and without I_{KACH} gradient the APD gradient was decreased to 28% (see Figure 2 and Table 2).

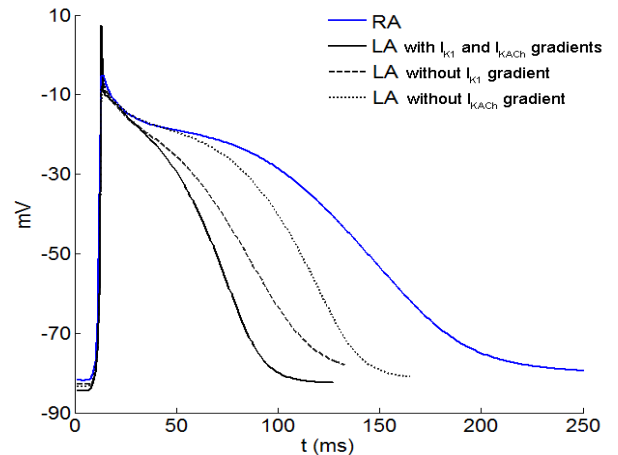


Figure 2. LA and RA action potentials in the pAF models. Table 2. APD₉₀ values in the center of LA and RA for the three different pAF models.

Model	APD ₉₀ (ms)	
	LA	RA
pAF	92	194
pAF without I _{K1} gradient	119	194
pAF without I _{KACH} gradient	139	194

In the pAF model (with both I_{KACH} and I_{K1} gradients) reentrant activity was initiated as a rotor in the posterior wall of the LA; following a hypermeandering trajectory and turning clockwise direction. Collisions and fragmentations were observed in some other LA regions. At 1800 ms the rotor was fragmented in two daughter waves, each one flanked by a singular point, inducing a figure-of-eight reentry in the posterior and inferior walls of the LA. At 2700 ms one of figure-of-eight reentry vortices was stabilized and converted in a rotor. During the remaining simulation, the rotor was converted in a figure-of-eight reentry and next transformed in a rotor following a hypermeandering trajectory in posterior and inferior wall of LA. In the RA, regular activity was observed. Flat fronts and some collisions between two flat fronts were observed during all simulation (Figure 3A).

In the pAF model without I_{K1} gradient, the AF episode was maintained by chaotic activity in the RA. Multiple reentries, rotors, fragmentations and collisions were observed in RA during all simulation. In the LA, regular activity was observed. Flat fronts and some collisions between two flat fronts were observed during all simulation (Figure 3B). In the pAF model without I_{KACH} gradient, the AF episode was also maintained by chaotic activity in the RA. Multiple reentries, rotors, fragmentations and collisions were observed in RA

during all simulation. In the LA, a rotor in the superior wall near to superior left pulmonary vein was generated, moving down towards the posterior wall until 1500ms. Next, regular activity was observed in the LA, flat fronts came from RA were observed during all simulation (Figure 3C).

In the pAF model (with both I_{KACH} and I_{K1} gradients) most of the RA points had DF values around 7 Hz whereas most of the LA points had DF values around 11 Hz. In contrast, in the pAF model without I_{K1} gradient and in the pAF model without I_{KACH} gradient, both atria showed DF values around 7 Hz and 6Hz, respectively (see the spectral analysis of electrograms calculated in the center of LA and RA in Figure 3).

4. Discussion

In this study we have observed that: (1) during pAF with I_{KACH} and I_{K1} gradients, a rotor and a figure-of-eight reentry sustained in the LA maintained the AF. (2) During pAF without I_{KACH} or I_{K1} gradients, multiple reentrant waves sustained in the RA maintained the AF. (3) LA-RA gradients in both I_{KACH} and I_{K1} expression are important in establishing LA-RA DF gradients during pAF.

4.1. Action potentials in the pAF models

Our results showed LA-RA APD gradient in all pAF models developed. Without I_{K1} or I_{KACH} gradients, the APD gradient decreases.

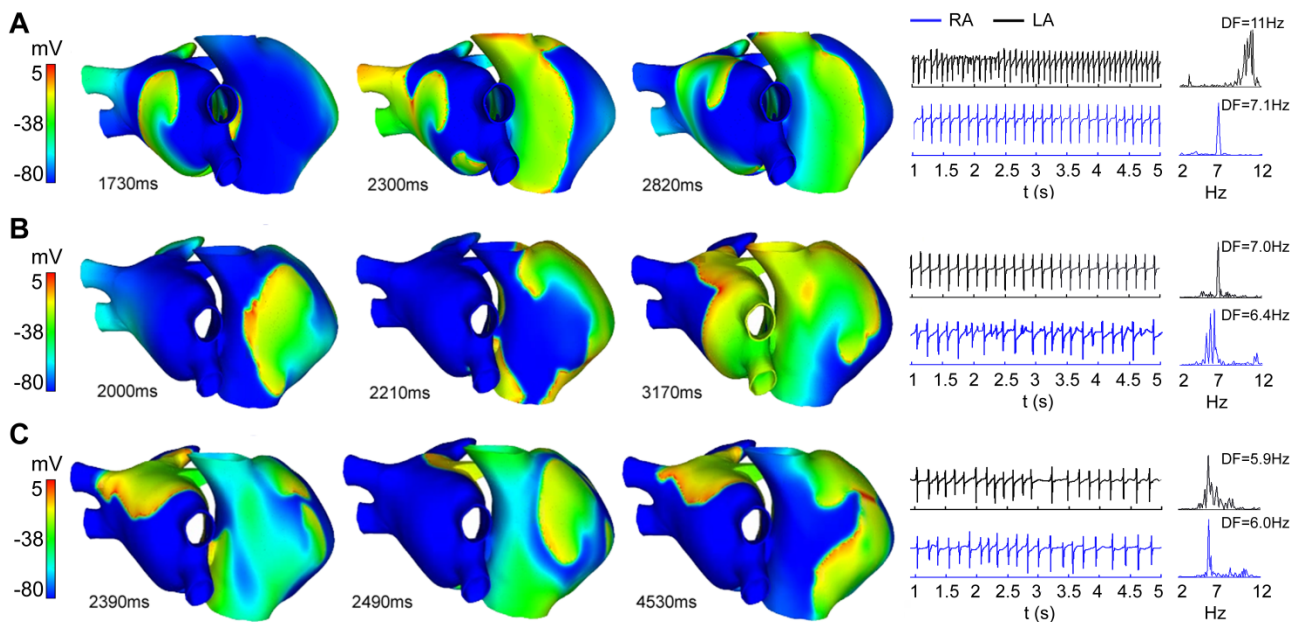


Figure 3. Propagation dynamics in A) pAF with I_{K1} and I_{KACH} gradients, B) pAF without I_{K1} gradient and C) pAF without I_{KACH} gradient. Electrograms calculated in the centre of LA and RA, and their spectrums are showed.

4.2. pAF dynamic

APD differences alone are insufficient to explain the mechanism of AF maintenance and the effects on pAF dynamic. Therefore our hypothesis is that during pAF, both ACh perfusion increasing the $I_{K_{ACh}}$ current in LA, and the I_{K1} increases in LA, as has been demonstrated by Voigt et al. [2], are capable of abbreviating atrial APD to extreme values are necessary for the arrhythmia to be established and maintained in LA.

Mansour et al. [11] and Sarmast et al. [3] in sheep hearts showed that increasing the ACh concentration increased the frequency of the dominant source (rotor), as well as the LA-RA frequency gradient, suggesting that the LA and RA are different in their response to ACh. Sarmast et al. [3] suggested that a heterogeneous response to cholinergic input cause a larger activation in the LA than in the RA, which sets the stage for the development of AF by it greatly abbreviates APD, and thus leads to an increase in the frequency of reentrant sources [12]. This allows stabilization of a dominant rotor in the region of greatest APD abbreviation (LA). However, our results suggest that it happens when both I_{K1} and $I_{K_{ACh}}$ gradients are present in the human atria. When I_{K1} or $I_{K_{ACh}}$ gradient does not exist, APD abbreviation in LA is not sufficient to allow stabilization of a dominant reentry (rotor or figure-of-eight reentry) in LA. In these cases, multiple reentrant waves sustained in the RA maintained the AF. Our hypothesis is that the terminal crest in RA and the electrophysiological heterogeneity in this area facilitate the maintenance of reentrant circuits in RA that collide and fragment, when a source is not stabilized in LA.

LA-RA DF gradients are much clearer in patients with pAF than those with permanent AF [11,13]. The ionic expression gradients could determine LA-RA DF gradients and rotor dynamics during pAF. In our simulations, LA-RA gradients in both $I_{K_{ACh}}$ and I_{K1} expression are important in establishing LA-RA DF gradients during pAF

5. Conclusion

In the pAF model, LA-RA gradients in both $I_{K_{ACh}}$ and I_{K1} expression are important in establishing APD gradients, LA-RA DF gradients and LA reentrant activity maintaining pAF.

Acknowledgements

This work was partially supported by the Programa Prometeo (PROMETEO/2012/030) of the Conselleria d'Educació Formació i Ocupació, Generalitat Valenciana and by the "VI Plan Nacional de Investigación Científica, Desarrollo e Innovación Tecnológica" from the Ministerio de Economía y Competitividad of Spain

(TIN2012-37546-C03-01) and the European Commission (European Regional Development Funds – ERDF - FEDER).

References

- [1] Kannel WB. Potency of vascular risk factors as the basis for antihypertensive therapy. *Eur Heart J* 1992;13(Suppl G):34-42.
- [2] Voigt N, Trausch A, Knaut M, et al. Left-to-right atrial inward rectifier potassium current gradients in patients with paroxysmal versus chronic atrial fibrillation. *Circ Arrhythm Electrophysiol* 2010;3(5):472-80.
- [3] Sarmast F, Kollí A, Zaitsev A, et al. Cholinergic atrial fibrillation: $I_{K_{ACh}}$ gradients determine unequal left/right atrial frequencies and rotor dynamics. *Cardiovasc Res* 2003;59(4):863-73.
- [4] Tobón C, Ruiz-Villa CA, Heidenreich E, et al. A three-dimensional human atrial model with fiber orientation. Electrograms and arrhythmic activation patterns relationship. *PLoS One* 2013;8(2):e50883.
- [5] Sanchez-Quintana D, Anderson RH, Cabrera JA, et al. The terminal crest: morphological features relevant to electrophysiology. *Heart* 2002;88(4):406-11.
- [6] Courtemanche M, Ramirez RJ, Nattel S. Ionic mechanisms underlying human atrial action potential properties: insights from a mathematical model. *Am J Physiol* 1998;275(1 Pt 2):H301-21.
- [7] Kneller J, Zou R, Vigmond EJ, et al. Cholinergic atrial fibrillation in a computer model of a two-dimensional sheet of canine atrial cells with realistic ionic properties. *Circ Res* 2002;90(9):E73-87.
- [8] Feng J, Yue L, Wang Z, et al. Ionic mechanisms of regional action potential heterogeneity in the canine right atrium. *Circ Res* 1998;83(5):541-51.
- [9] Boineau JP, Canavan TE, Schuessler RB, et al. Demonstration of a widely distributed atrial pacemaker complex in the human heart. *Circulation* 1988;77(6):1221-37.
- [10] Li D, Zhang L, Kneller J, et al. Potential ionic mechanism for repolarization differences between canine right and left atrium. *Circ Res* 2001;88:1168–75.
- [11] Mansour M, Mandapati R, Berenfeld O, et al. Left-to-right gradient of atrial frequencies during acute atrial fibrillation in the isolated sheep heart. *Circulation* 2001;103(21):2631-6.
- [12] Shumaker JM, Clark JW, Giles WR. Simulations of passive properties and action potential conduction in an idealized bullfrog atrial trabeculum. *Math Biosci* 1993;116:127–67.
- [13] Sanders P, Berenfeld O, Hocini M, et al. Spectral analysis identifies sites of high frequency activity maintaining atrial fibrillation in humans. *Circulation* 2005;112:789-797.

Address for correspondence.

Catalina Tobón Zuluaga.
Calle 2 Sur No 20-185 apto 1803, Medellín, Colombia.
ctobon@gbio.i3bh.es.